# Fabrication and characterization of photocatalytic activity of Fe$_3$O$_4$-doped CdS hollow spheres

Wanquan Jiang [a,*], Cuifeng Jiang [a], Zhen Cao [a], Xinglong Gong [b,*], Zhong Zhang [c]

[a] Department of Chemistry, Hefei 230026, PR China
[b] CAS Key Laboratory of Mechanical Behavior and Design of Materials, Department of Modern Mechanics, University of Science and Technology of China, Hefei 230027, PR China
[c] National Center for Nanoscience and Technology, Beijing 100080, PR China

## ARTICLE INFO

## ABSTRACT

A new hollow sphere photocatalyst has been fabricated by combining Fe$_3$O$_4$ with nanoparticulate CdS. Their microstructures and photocatalytic behavior were examined by X-ray powder diffraction, transmission electron microscope, scanning electron microscope and ultraviolet and visible spectroscopy. These hollow nanostructures displayed superparamagnetism at room temperature. It showed higher activity on hollow sphere than solid particle as the catalysis result.

© 2009 Elsevier Ltd. All rights reserved.

## 1. Introduction

With the rapid development of dyestuff industry, printing dye wastewater has already become one of the most significant pollution sources of water environment. This pollution source has attracted much attention of the society and therefore extensive and intensive research work was attempted to solve this problem. For example, the application of semiconductor catalysts for degradation of organic pollution has been a key global research hotspot recently [1–6]. It is mainly because this approach does not generate any secondary pollution by making use of solar energy. Although possessing advantages of stability and low cost, the semiconductor catalyst has been proved to be of somewhat limited use owing to the difficulties in separating the products and residual catalysts [7]. The immobilization of semiconductor catalyst has therefore attracted a lot of attention.

Inorganic nanoporous materials utilized as catalyst supports for many homogeneous catalysts have been successfully demonstrated [8–13]. Among various support materials, magnetic nanoparticles have become the prominent candidates due to their unique properties and potential applications in various fields [14–20], especially the regathering and recycling of expensive catalysts [7]. Magnetic separation has always been a convenient method for separating magnetized species easily and thoroughly from the multiphase system by a simple magnetic device without

centrifugation or filtration [7]. This approach can increase the durability of the catalysts and be operated easily in industry. For example, magnetic nanoparticles utilized for removing and recycling catalysts have been successfully demonstrated [7,21].

Unfortunately, since magnetic nanoparticles themselves have strong magnetic properties and could easily aggregate together, pursuing satisfactory dispersion has been a critical problem [22]. To tackle this problem, magnetic hollow sphere catalysts have been fabricated to improve dispersity by decreasing catalyst density [23]. Herein, fabrication of Fe$_3$O$_4$-doped CdS hollow sphere through a simple wet-chemistry method is reported in this paper. Comparison of photocatalytic activity between hollow and solid nanoparticles has been investigated.

## 2. Experimental procedure

### 2.1. Preparation of PSA@Fe$_3$O$_4$

The material components include: cadmium acetate (99.9%, CR), tetrahydrofuran (THF) and ammonium hydroxide (NH$_3 \cdot$ H$_2$O, 25–28%) obtained from Lingfeng Chemical Reagent Co., Ltd. of Shanghai. Ferric chloride hexahydrate (AR), sodium sulfite anhydrous (AR), thioacetamide (TAA, AR) and methyl orange (MO) were obtained from Sinopharm Chemical Reagent Co., Ltd. All substances were used without further purification.

The PSA@Fe$_3$O$_4$ composites were prepared by a simple wet-chemistry method reported previously [24]. In a typical synthesis, PSA was dispersed in a blend solution with a volume ratio of 2:1

* Corresponding authors. Tel.: +86 551 3607605; fax: +86 551 3600419.
E-mail addresses: jiangwq@ustc.edu.cn (W. Jiang), gongxl@ustc.edu.cn (X. Gong).

($V_{ethanol}$:$V_{water}$ = 2:1) and 50 mL of $FeCl_3 \cdot 6H_2O$ (0.006 mol/L) which had been purged with nitrogen for 20 min to remove all traces of oxygen that was added. After stirring for 20 min, $Na_2SO_3$ (0.001 mol/L) aqueous solution was gradually added under stirring, followed by a dropwise addition of $NH_3 \cdot H_2O$ to adjust the pH value to 8. The mixture was stirred for 3 h at 65 °C under nitrogen atmosphere. After being separated by a magnetic field, the PSA@$Fe_3O_4$ precipitate was obtained.

## 2.2. Preparation of $Fe_3O_4$-doped CdS hollow spheres

The synthesis of magnetic catalyst is as follows: typically, the as-prepared magnetic substrate particles were dissolved in 40 mL of $Cd(CH_3COO)_2 \cdot 2H_2O$ (0.05 mol/L) solution. 30 mmol/L of thioacetamide was then added .The mixture had a very clear reaction with gradually deepened yellow colour, indicating the formation of CdS. The mixture was then stirred for 12 h at 65 °C. The coating process was repeated twice. Finally, the PSA@$Fe_3O_4$-doped CdS composites were separated.

The composite particles were converted to $Fe_3O_4$-doped CdS hollow capsules after being soaked in THF. Subsequently, the resulting hollow spheres were washed with water and ethanol, then, they were dried at 50 °C for 4 h under vacuum.

## 2.3. Photocatalytic testing of the obtained $Fe_3O_4$-doped CdS hollow capsules

The photocatalytic activity of the samples was measured by the decomposition of MO in an aqueous solution. The UV light was generated by a 400 W high-pressure hydrargyrum lamp. Prior to irradiation, the suspension containing a powdered catalyst (300 mg) and fresh aqueous solution of MO was sonicated for 10 min. Given irradiation time intervals, a series of aqueous solutions in a certain volume were collected and separated by a magnetic field to remove the catalyst composites. The photocatalytic performance of the catalyst was evaluated by monitoring the visible absorbance (at $\lambda_{max} = 463$ nm) characteristic of the target MO through UV–vis spectroscopy using a Shimadzu UV-2401PC spectrometer.

## 2.4. Characterization

X-ray powder diffraction (XRD) patterns of the products were obtained with a Japan Rigaku D/Max-γA rotation anode X-ray diffractometer equipped with graphite monochromatized Cu $K_\alpha$ radiation ($\lambda = 0.154178$ nm). Transmission electron microscopy (TEM) photographs were taken with a Hitachi model H-800 transmission electron microscope at an accelerating voltage of 200 kV. Scanning electron microscopy (SEM) images were explored with a JSM-6700F Field Emission, Scanning Electron Microanalyser. The nitrogen ($N_2$) adsorption/desorption isotherms at about 77 K were studied dispending Micromeritics, ASAP 2020 M system. The optical absorption was recorded by an ultraviolet–visible (UV)-2401(PC)S manufactured by Shimadzu Corporation. The magnetization curves ($M–H$ curve) of the samples were recorded with a Physical Properties Measurement System supplied by the Quantum Design Corporation. The stability of the photocatalyst was determined by measuring the amount of cadmium in processed water. The solution was diluted and the cadmium concentration was determined by inductively coupled plasma atomic emission spectroscopy (ICP–AES) (Atomscan Advantage supplied by the Thermo Jarrell Ash Corporation).

## 3. Results and discussion

The crystal structures of the prepared composites were observed by the XRD measurement. A typical XRD pattern of PSA@$Fe_3O_4$ is shown in Fig. 1a, in which the diffraction peaks correspond to $Fe_3O_4$ [25]. It can be observed that a characteristic peak appears at $2\theta = 20.3°$ for PSA [26]. From Fig. 1b, it can be deduced that the composites are composed of crystalline $Fe_3O_4$ and CdS, while diffraction peaks can be indexed to a typical bulk cubic CdS with the cell parameters $a = 5.406$ Å. This is consistent with the standard value for bulk cubic CdS (JCPDS 80-0019). When the composites were treated in THF, the change of the characteristic peaks of $Fe_3O_4$ and CdS cannot be observed. The particle size of the shell is roughly estimated as 30 nm with the Scherrer's equation [27], while in accordance to SEM, the shell is about 35–45 nm. That is because Scherrer's equation gives the original size, while aggregation exists in the SEM. No diffraction peaks from other crystalline forms are detected, which demonstrates that these hollow $Fe_3O_4$-doped CdS samples have high purity and crystallinity.

The $Fe_3O_4$-doped CdS hollow sphere was further subjected to TEM and SEM analysis (Fig. 2). The TEM image in Fig. 2a shows that the magnetite nanoparticles occupy only a fraction of the volume of PSA core. Comparing Fig. 2b with Fig. 2a, it is clear that CdS has been successfully coated on the PSA@$Fe_3O_4$ composite. The hollow structure of the spheres is clearly revealed from the TEM image shown in Fig. 2c compared with Fig. 2b. It is evident that there is a strong contrast difference in all of the spheres with dark edge and bright center, confirming their hollow structure [28]. The broken spheres (arrows point to) obtained from SEM (Fig. 2d) indicate hollow structures further. Thioacetamide, a nonionic precursor, was chosen as the starting material. The $S^{2-}$ ions, produced with a slow speed in alkaline solution and under the heat treatment results in the slow growth of the nanocrystal CdS [29,30]. Therefore, homogeneous CdS shell was obtained. We speculate that the PSA core was dissolved in THF forming a hollow sphere.

$$CH_3CSNH_2 + 2OH^- \text{—} CH_3COO^- + NH_4^+ + S^{2-}$$

Nitrogen adsorption–desorption isotherms are measured to determine the specific surface area and pore volume of the $Fe_3O_4$-doped CdS hollow microspheres, and the corresponding results



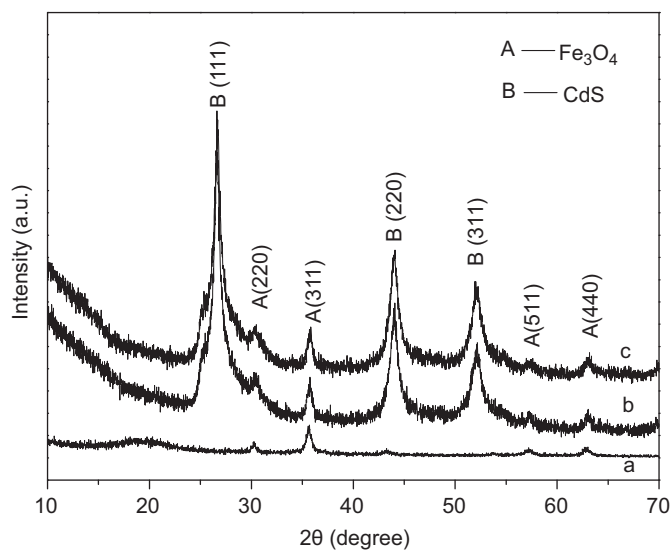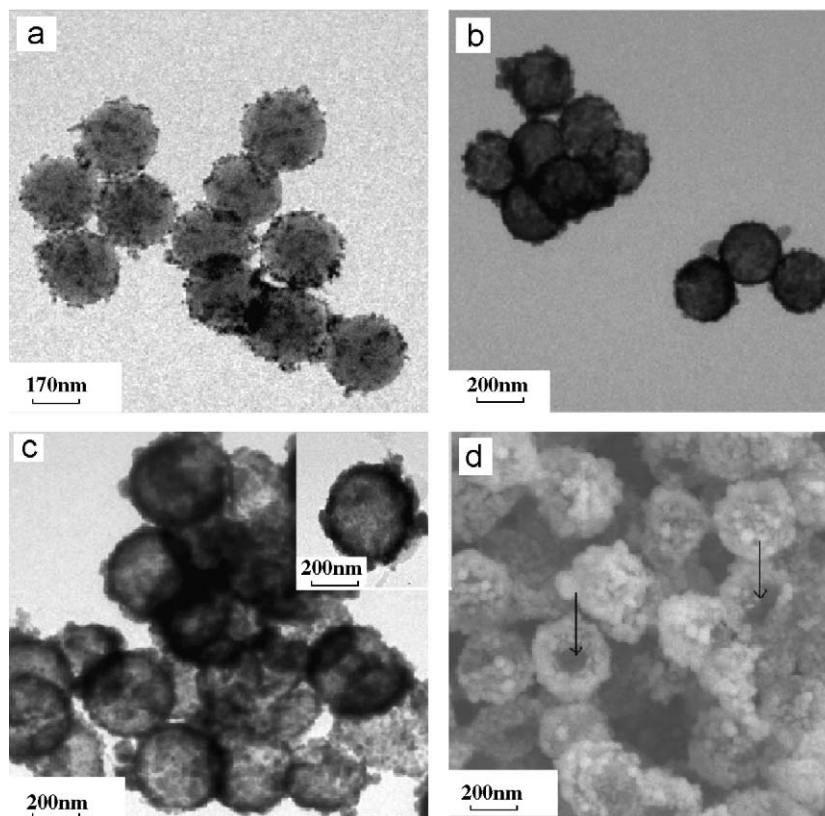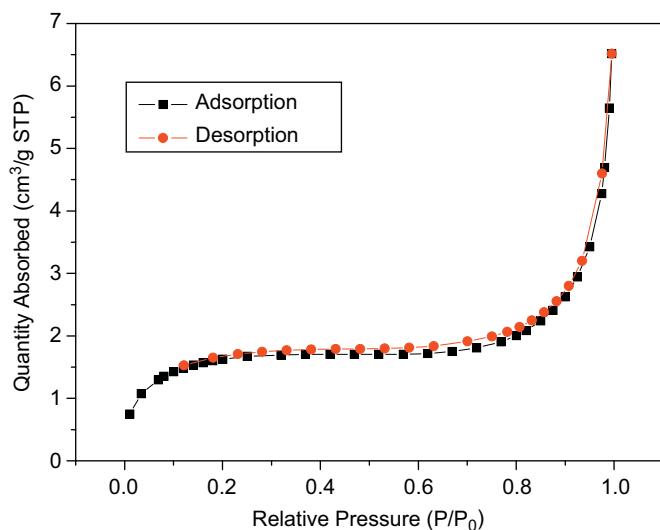Fig. 1. X-ray diffraction patterns of (a) PSA@$Fe_3O_4$; (b) PSA@$Fe_3O_4$-doped CdS and (c) $Fe_3O_4$-doped CdS hollow spheres.
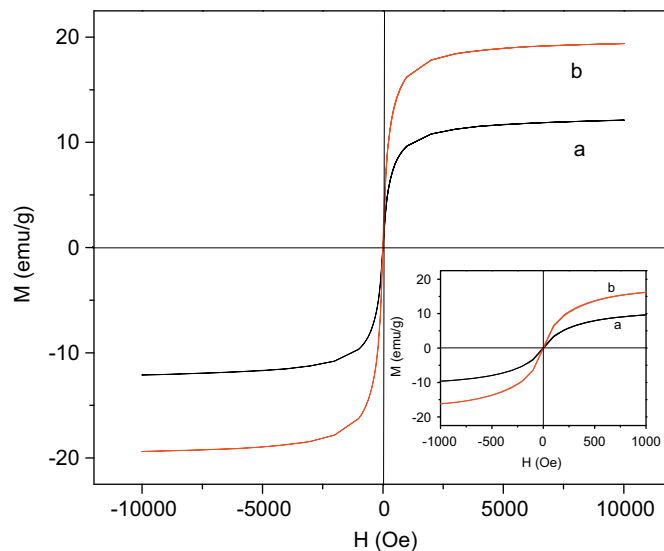
**Fig. 2.** TEM of (a) PSA@$Fe_3O_4$; (b) PSA@$Fe_3O_4$-doped CdS and (c) $Fe_3O_4$-doped CdS hollow spheres and SEM of $Fe_3O_4$-doped CdS hollow spheres.



**Fig. 3.** Nitrogen adsorption–desorption isotherm of the $Fe_3O_4$-doped CdS hollow microspheres.



**Fig. 4.** Room-temperature magnetization curve of (a) PSA@$Fe_3O_4$-doped CdS and (b) $Fe_3O_4$-doped CdS particles.

are presented in Fig. 3. The isotherms are typical type IV, which indicates the presence of mesoporous and macroporous materials according to IUPAC classification [31]. The BET surface area and pore volume of the hollow microspheres are 5.90 m²/g and 0.23 cm³/g, respectively, which means there are a few small pores on the surface, that allow the MO solution to come into the hollow sphere.

The $M(H)$ curves of the samples are shown in Fig. 4, in which the nanoparticles exhibit a superparamagnetic behavior without the observation of coercivity and remanence. These facts are related to finite size and surface effects [32]. The superparamagnetic behavior shows the potential applications in magnetic devices on the nanometer scale. The saturation magnetization of this magnetite nanoparticles is 18 emu/g, which is bigger than the reported value 3.69 emu/g of 27 nm magnetite nanoparticles [33]. Thus, the high saturation magnetization in this case probably attributes to the big size of $Fe_3O_4$ nanoparticles.
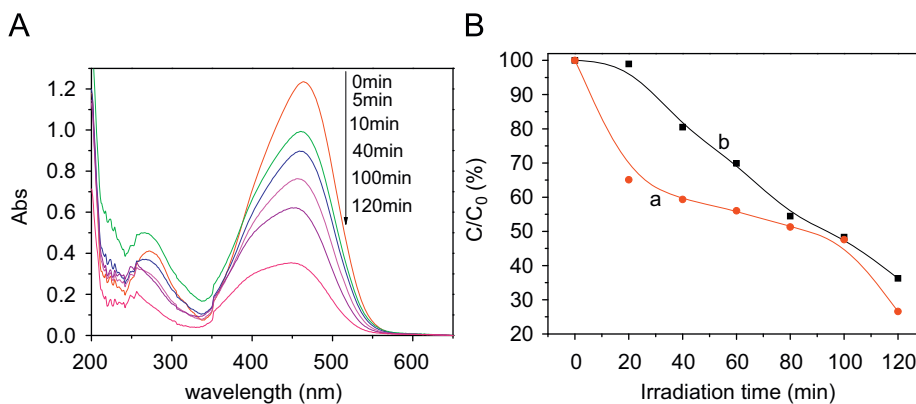
**Fig. 5.** (A) UV–vis spectroscopy of MO at different times in the photocatalytic experiment and (B) effect of illumination time on the degradation of MO when using different catalysts (a) PSA@$Fe_3O_4$-doped CdS and (b) $Fe_3O_4$-doped CdS.

According to previous results [1,4], CdS semiconductor can exhibit catalysis on organic dyes and therefore research about the catalysis of the magnetic composite has been performed. Photocatalytic activity of the resulting samples was investigated on the degradation of MO in an aqueous solution. The relation between MO reduction ratio ($C/C_0$) and light application time is shown in Fig. 5B. It has been observed that the reduction of MO by PSA@$Fe_3O_4$ did not occur to an appreciable extent without CdS nanoparticles, indicating that CdS nanoparticles play the role of a catalyst for the reduction of MO.

As expected, enhanced photocatalytic properties of the hollow composite (Fig. 5B-b) were observed comparing to that of PSA@$Fe_3O_4$-doped CdS (Fig. 5B-a). This fact can be explained as follows. The catalytic activity could be reduced due to a decrease in the surface area deduced by the collision and amalgamation of CdS particles during the photocatalysis reaction [34], while the possibility of particle collision and amalgamation decreases in $Fe_3O_4$-doped CdS catalyst because of better dispersion as a result of smaller density. Consequently, higher photocatalytic activity is obtained. In Fig. 5B, the degradation percent between 100 and 120 min is deviant. After preliminary analysis, the most likely cause of the deviance is that, after 100 min irradiation, part of photocatalyst began to gather, which induced the irregular photocatalysis plot line. On the other hand, the sample has been degraded 50%; hence, it is more difficult for the photocatalyst to be in collision with MO.

In order to find the stability of the photocatalyst, the processed water was conducted ICP–AES analysis after catalysis reaction. As a result, it was found that about 0.1% CdS was in the solution, which means 99.9% CdS was stable enough to stay attached to the PSA@$Fe_3O_4$.

Obviously, the photodegradation of MO concentration is up to 75% which is achieved in the $Fe_3O_4$-doped CdS hollow spheres suspension after 120 min irradiation. This novel magnetic hollow sphere photocatalyst is expected to find applications in many other industrially important catalytic processes.

## 4. Conclusion

In conclusion, a new magnetic hollow sphere photocatalyst for degradation of organic dyes based on magnetite nanoparticles incorporated in CdS nanoparticles has been prepared. It was found that the as-prepared hollow composite displayed superparamagnetic property. The studies suggest higher photocatalytic ability on $Fe_3O_4$-doped CdS hollow particles compared to solid particles because of larger surface area. The photodegradation of MO

concentration is up to 75% which is achieved in the hollow sphere water suspension after 120 min irradiation.

## References

[1] A. Datta, A. Priyam, S.N. Bhattacharyya, K.K. Mukherjea, A. Saha, J. Colloid Interface Sci. 322 (2008) 128–135.
[2] S.S. Srinivasan, J. Wade, E.K. Stefanakos, J. Alloys Compd. 422 (2006) 322–326.
[3] M.W. Xiao, L.S. Wang, Y.D. Wu, X.J. Huang, Z. Dang, Nanotechnology 19 (2008) 015706.
[4] J.B. Chen, S. Lin, G.Y. Yan, L.Y. Yang, X.Q. Chen, Catal. Commun. 9 (2008) 65–69.
[5] J.K. Zhou, L. Lv, J.Q. Yu, H.L. Li, P.Z. Guo, H. Sun, X.S. Zhao, J. Phys. Chem. C 112 (2008) 5316–5321.
[6] Y. Wang, Y. Wang, Y.L. Meng, H.M. Ding, Y.K. Shan, X. Zhao, X.Z. Tang, J. Phys. Chem. C 112 (2008) 6620–6626.
[7] M. Shokouhimehr, Y.Z. Piao, J. Kim, Y.J. Jang, T. Hyeon, Angew. Chem., Int. Ed. 46 (2007) 7039–7043.
[8] J.A. Melero, R.V. Grieken, G. Morales, Chem. Rev. 106 (2006) 3790–3812.
[9] A. Corma, H. Garcia, Adv. Synth. Catal. 348 (2006) 1391–1412.
[10] J.S. Chang, S.H. Jhung, Y.K. Hwang, S.E. Park, J.S. Hwang, Int. J. Nanotechnol. 3 (2006) 150–180.
[11] D.R. Rolison, Science 299 (2003) 1698–1701.
[12] M.E. Davis, Nature 417 (2002) 813–821.
[13] S.J. Bae, S.W. Kim, T. Hyeon, B.M. Kim, Chem. Commun. (2000) 31–32.
[14] A.H. Lu, E.L. Salabas, F. Schüth, Angew. Chem., Int. Ed. 46 (2007) 1222–1244.
[15] S. Morent, S. Vasseur, F. Grasset, E. Duguet, J. Mater. Chem. 14 (2004) 2161–2175.
[16] Q.A. Pankhurst, J. Connolly, S.K. Jones, J. Dobson, J. Phys. D: Appl. Phys. 36 (2003) R167–R168.
[17] O. Sato, J. Tao, Y.Z. Zhang, Angew. Chem., Int. Ed. 46 (2007) 2152–2187.
[18] T. Hyeon, Chem. Commun. (2003) 927–934.
[19] H.W. Gu, P.L. Ho, K.W.T. Tsang, L. Wang, B. Xu, J. Am. Chem. Soc. 125 (2003) 15702–15703.
[20] J. Won, M. Kim, Y.W. Yi, Y.H. Kim, N. Jung, T.K. Kim, Science 309 (2005) 121–125.
[21] [a] J.J. Xu, Y.H. Ao, D.G. Fu, C.W. Yuan, J. Phys. Chem. Solids 69 (2008) 1980–1984;
   [b] T.J. Yoon, W. Lee, Y.S. Oh, J.K. Lee, New J. Chem. 27 (2003) 227–229;
   [c] A.N. Ajjou, H. Alper, J. Am. Chem. Soc. 120 (1998) 1466–1468;
   [d] Y.M. Chung, K.K. Kang, W.S. Ahn, P.K. Lim, J. Mol. Catal. A: Chem. 137 (1999) 23–29;
   [e] J.H. Chen, H. Alper, J. Am. Chem. Soc. 119 (1997) 893–895.
[22] X.J. Ding, T.C. An, G.Y. Li, S.Q. Zhang, J.X. Chen, J.M. Yuan, H.J. Zhao, H. Chen, G.Y. Sheng, J.M. Fu, J. Colloid Interface Sci. 320 (2008) 501–507.
[23] F. Caruso, M. Spasova, A. Susha, M. Giersig, R.A. Caruso, Chem. Mater. 13 (2001) 109–116.
[24] C.F. Jiang, M.W. Chen, S.H. Xuan, W.Q. Jiang, X.L. Gong, Z. Zhang, Can. J. Chem. 87 (2009) 502–506.
[25] P.H. Wang, C.Y. Pan, Colloid Polym. Sci. 280 (2002) 152–159.
[26] H.P. Klug, L.E. Alexander (Eds.), Wiley, New York, 1962, p. 491.

[27] S.C. Qu, H.B. Yang, D.W. Ren, S.H. Kan, G.T. Zou, D.M. Li, M.H. Li, J. Colloid Interface Sci. 215 (1999) 190–192.

[28] J.S. Hu, Y.G. Guo, H.P. Liang, L.J. Wan, C.L. Bai, Y.G. Wang, J. Phys. Chem. B 108 (2004) 9734–9738.

[29] S.Q. Sun, T. Li, Cryst. Growth Des. 7 (2007) 2367–2371.

[30] S.H. Liu, H.W. Lu, X.F. Qian, J. Yin, Z.K. Zhu, J. Solid State Chem. 172 (2003) 480–484.

[31] K.S.W. Sing, D.H. Everett, R.A.W. Haul, L. Moscou, R.A. Pierotti, J. Rouquérol, T. Siemienie- wska, Pure Appl. Chem. 57 (1985) 603–619.

[32] T.Z. Yang, C.M. Shen, H.T. Yang, G.W. Xiao, Z.C. Xu, S.T. Chen, D.X. Shi, H.J. Gao, Surf. Interface Anal. 38 (2006) 1063–1067.

[33] Y.H. Zheng, Y. Cheng, F. Bao, Y.S. Wang, Mater. Res. Bull. 41 (2006) 525–529.

[34] H. Fujii, M. Ohtaki, K. Eguchi, H. Arai, J. Mol. Catal. A: Chem. 129 (1998) 61–68.